ON PRESSURE MEASUREMENT IN A VOLUME WITH UNSTEADY PROCESSES

V.P. Zamuraev and A.F. Latypov

Institute of Theoretical and Applied Mechanics, SB RAS
630090 Novosibirsk, Russia

Probes for pressure measurement in a pulse wind tunnels prechamber or in a ramjet combustion chamber are posed usually in face of a narrow duct adjoined to the tested volume. Therewith, the pressure depends essentially on length of the used duct. At quick unsteady processes the pressure in long ducts is widely "smeared" in time, and the pressure in short ducts has an oscillating character. At that, a question on correspondence of a measured pressure to a real pressure in volume arises. This paper considers the problem for short ducts in the frames of the Euler equations.

Problem formulation

Development of disturbances in closed chamber by local momentary energy release is considered. The chamber is planar and has a rectangular form. The narrow duct adjoins perpendicular to the chamber wall. The disturbance develops, reaches the duct and enters it. The duct bottom pressure begins to change in time. To simulate a disturbance development in gas with a constant ratio of specific heat γ, the Euler equations in conservative form are solved:

$$\partial \boldsymbol{U}/\partial t + \partial \boldsymbol{F}/\partial x + \partial \boldsymbol{G}/\partial y = 0,$$

$$\boldsymbol{U} = (\rho,\ \rho u,\ \rho v,\ e),\ \boldsymbol{F} = (\rho u,\ p+\rho u^2,\ \rho uv,\ u(p+e)),\ \boldsymbol{G} = (\rho v,\ \rho uv,\ p+\rho v^2,\ v(p+e)).$$

Here the x and y coordinates are directed along and across the chamber correspondingly and are normalized to its width d; the time t is normalized to d/a_0, the gas velocity components u and v and the velocity of sound a to a_0, the density ρ to ρ_0 (the initial gas density is equal to $\gamma\rho_0$); the pressure p and the total energy of a gas volume unit e are normalized by the value $\rho_0 a_0^2$; p_0 and a_0 – undisturbed dimensional pressure and velocity of sound in the chamber. For the considered gas model, we have

$$p = (\gamma - 1)\cdot(e - \rho\,(u^2 + v^2)/2), \quad a^2 = \gamma p/\rho\ .$$

To solve these equations, the no-slip condition is set at the chamber and duct walls: $v_n = 0$, where v_n is a normal velocity component. At the initial moment of time the gas is at rest ($u = v = 0$), and in the whole region, except a small energy release zone, the gas parameters are undisturbed. The energy release zone is placed inside the chamber and has a rectangular form ($l_1 \le x \le l_2$, $d_1 \le y \le d_2$). It is considered that energy release is very quick and the gas density in the corresponding period of time is not changed, only the local pressure and temperature are changed. A higher initial pressure is set in this zone. The corresponding temperature is determined from a condition of the energy release at the constant volume. The other parameters (ρ, u, v) are the same as in the rest part of the flow domain. The narrow duct adjoins to the chamber at $l_3 \le x \le l_4$, $y = 0$, its length is d_k. The momentary and mean in time bottom pressure, dependence on time of the mean gas characteristics and relative fluctuations of these values are calculated. This task simulates the pressure measurement.

Numerical method

For numerical solution of the given problem the McCormack method [1] in combination with a grid procedure offered in [2, 3] is used. This method allows to introduce grids with a step

Report Documentation Page

Report Date	Report Type	Dates Covered (from... to)
23 Aug 2002	N/A	-

Title and Subtitle On Pressure Measurements in A Volume With Unsteady Processes	**Contract Number**
	Grant Number
	Program Element Number
Author(s)	**Project Number**
	Task Number
	Work Unit Number
Performing Organization Name(s) and Address(es) Institute of Theoretical and Applied Mechanics Institutskaya 4/1 Novosibirsk 530090 Russia	**Performing Organization Report Number**
Sponsoring/Monitoring Agency Name(s) and Address(es) EOARD PSC 802 Box 14 FPO 09499-0014	**Sponsor/Monitor's Acronym(s)**
	Sponsor/Monitor's Report Number(s)

Distribution/Availability Statement
Approved for public release, distribution unlimited

Supplementary Notes
See also ADM001433, Conference held International Conference on Methods of Aerophysical Research (11th) Held in Novosibirsk, Russia on 1-7 Jul 2002

Abstract

Subject Terms

Report Classification unclassified	**Classification of this page** unclassified
Classification of Abstract unclassified	**Limitation of Abstract** UU

Number of Pages
8

by an order smaller in some subdomains. The given procedure does not cause oscillations and unphysical waves.

In brief, the essence of the suggested method is as follows. The whole flow domain in which the gas dynamic equations are numerically solved is separated into a number of subdomains successively encircling each other (in the present paper the flow domain is separated into two subdoamins). In each of them, a rectangular grid with the same direction of the cell sides is introduced. In the exterior subdomain the most coarse grid is built. In the inner subdomain including the release zone, the grid is the finest. The introduced grids do not overlap.

The steps in transition to a finer grid may considerably decrease, for example, by an order. The integration step with respect to time varies same-fold accordingly. Thus, the Courant criteria has the same value for all subdoamins, and in each the solution may be found according to the same difference scheme.

To connect the solutions, the subdomains are expanded to the neighboring ones. Two nodes layers of the coarse grid are introduced into subdomains with a fine grid near a bound with the coarse grid domain. The fine grid is extended into the coarse grid subdomain by one coarse step (under refinement relation r by r small steps). The flow parameters in additional nodes on the previous time layer are found according to the parameters in the parent grids nodes for the same moment of time. It is made by linear interpolation. The obtained parameter values are used as the boundary conditions to find the solutions in the subdomains in a new time layer.

Use of a linear interpolation makes some error into fluxes of mass, impulse and energy on the grids bounds. However, as it is shown in [3], error introduction into the difference scheme of a second order does not decrease its approximation order, and only leads to a weak violation of the conservatism of this method.

Further, according to the same difference scheme using hydrodynamic fluxes, gasdynamic parameters in a new time layer were calculated. It is performed independently in each subdomain. In the coarse grid subdomain only one time step Δt is made, whereas in the fine grid subdomain r steps are made, each is equal to $\Delta t/r$. A number of nodes in every expanded subdomain where new parameters are found are reduced from the side of another subdomain. As a result, in the new time layer the flow parameters become well-known in all subdomain nodes without expansion.

Tests conducted in [3] showed an effectiveness of the given numerical method.

Calculation results

The calculations are made for the following parent parameters: $p = 1$, $\rho = 1.4$, $u = v = 0$. Width and length of the chamber are equal $d = 1$, $l = 2$ accordingly. The energy release zone is determined by the values $l_1 = 1.10$, $l_2 = 1.15$ (in the main variant), $d_1 = 0.05$, $d_2 = 0.10$. The initial pressure in this zone is equal to $p = 100$, 1000, 10000. The narrow duct adjoins to the chamber at $1.10 \le x \le 1.15$, $y = 0$ in the main variant (in the additional variant $1.175 \le x \le 1.225$, $y = 0$); The duct length is $d_k = 0.2$. At that, it were performed the calculations at the value of the supplied energy $\Delta E = 62.5$ and at different longitudinal size of the energy release zone. This size took the value as $\Delta x = 0.05$, 0.2, 0.4, 0.5 and 1 (the supplied energy density is inversely proportional to Δx).

Figure 1, *a* and *b*, corresponding to the main and additional variants, show the pressure field on the initial stage ($t = 0.012$) of the disturbance development caused by the energy release ($p = 1000$). Isobars $p = 2$, 10 and further with a step 10 up to 90 give a concept of the shock waves system, rarefaction waves and other phenomena arisen by momentary local energy release. Pressure distribution (Fig. 1, *a*) is symmetrical with respect to the vertical line when it passes a center of the energy release zone. Analogous distribution (Fig. 1, *b*) is strongly unsymmetrical in the low part of the disturbance domain. It is caused by a shift of the narrow duct

relatively to the energy release zone. The shock wave falling from the energy release zone to the narrow duct, reflects from the low chamber wall and from the duct side wall. The shock wave entering the narrow duct, propagates over it, and it does not attenuate. The pressure behind the wave (Fig. 1, *a*) is above 60. The pressure behind the wave reflected from the duct bottom becomes significantly higher. At the same time, the shock wave propagating from the energy release zone in the chamber constantly attenuates. In the considered moment of time (Fig. 1, *a*) the pressure behind it is somewhat higher than 40. In the central disturbance region including the energy release zone the gas pressure is lower than 30 because the gas flies away.

Distribution of the gas density is greatly non-uniform. It is shown in Fig. 2, *a* and *b* (the density is normalized to non-disturbace value). The parameters correspond to the conditions of Fig. 1, *a* and *b*. The density levels are as follows: 0.04, 0.05 (Fig. 2, *a*), 0.1 and further with a step 0.1 up to 0.6; then 0.8, 1.0 and with a step 0.5 up to 3.0. In the central part of the disturbance domain the gas density strongly falls because it flys away (in Fig. 2, *a* it is lower than 0,04, that is it falls more than 20 times in comparison with undisturbed value; in Fig. 2, *b* the density is somewhat lower 0.1). Difference in the values ρ of these two variants is connected with a position of the narrow duct which is placed more distant from the energy release zone. It is shown in Fig. 2, *b*. The region of minimum density values is slightly shifted to the upper wall. The character of parameter distribution in the initial moments of time corresponds qualitatively to the theory of strong explosion.

By the further disturbance development the shock wave reflection from the chamber walls is observed. Fig. 3 for the moment of time equal to t =0.3 shows a systems of isobars at the energy release ΔE = 62.5 in a narrow long zone (Fig. 3, *a* corresponds to the initial pressure in the region of the energy release p = 1250, Figure presents the isobars for the values p from 2 up to 22 with a step 1, then for p = 24, 25, 27.5, further from 30 up to 75 with a step 5, in the narrow duct the additional pressure levels 23 and 26 are shown; Fig. 3, *b* corresponds to the initial pressure in the energy release zone p = 500, Figure presents the isobars for the values p from 1 with a step 1 up to 15, and also for p = 17.5, further from 20 with a step 2 up to 30, then with a step 2.5 up to 40). Fig. 3, *a* shows the rarefaction waves which formation have been resulted from the shock wave reflection from the upper and side walls of the chamber by the considered moment of time: near the upper wall the pressure in the extensive region of the rarefaction waves is lower 3, and in the left and right bottom corners is lower than 2. In the left and right upper chamber corners the most complex system of the shock waves and the highest pressure ~ 75 are observed. The reflected shock wave passing inside the chamber is essentially weaker. In the narrow duct the pressure is ~26. The shock wave reflected from the bottom chamber wall (shock wave pressure is ~14) is seen in Fig. 3, *b*. At the left and at the right it is jointed with the shock waves reflected from the side chamber walls. Behind bottom part of these shock waves there are the rarefaction waves (in which the pressure decreases up to 1). At the left and right upper chamber corners the pressure behind the shock waves reaches 40. It is also observed the shock wave reflection from the upper chamber wall.

Further, very complex flow picture is observed in the result of multi-reflection from the chamber walls of relatively weak shock waves and rarefaction waves, of their interaction between each other, multi-entrance (and multi-exit) of the shock waves into the narrow duct. In consequence of this, an oscillating character of dependence of pressure on time at the narrow duct bottom is seen. It is shown in Fig. 4 for the main variant with the initial pressure in the energy release zone p = 10000.

Such dependence on time for measured pressure has been obtained in [4] by dynamical calibration of pneumatic routes whose length in the experiments were varied from 100 mm up to 1000 mm with diameter from 1 up to 3 mm. Air was previously evacuated from the pneumatic route up to the pressure of 0.11 atm. Atmospheric air enters the duct when the entrance was opened. If the pneumatic routes are of large length, the measured pressure was increased in

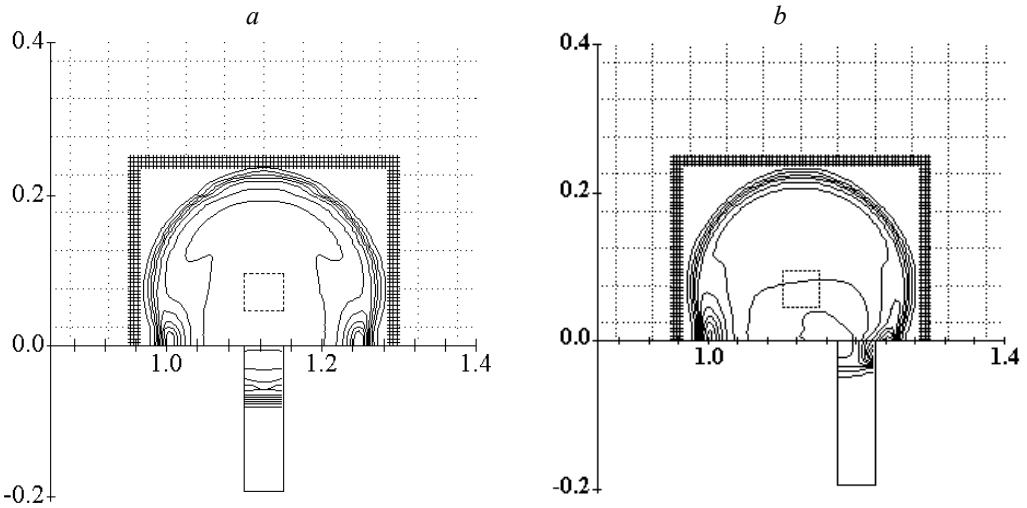

Fig. 1.

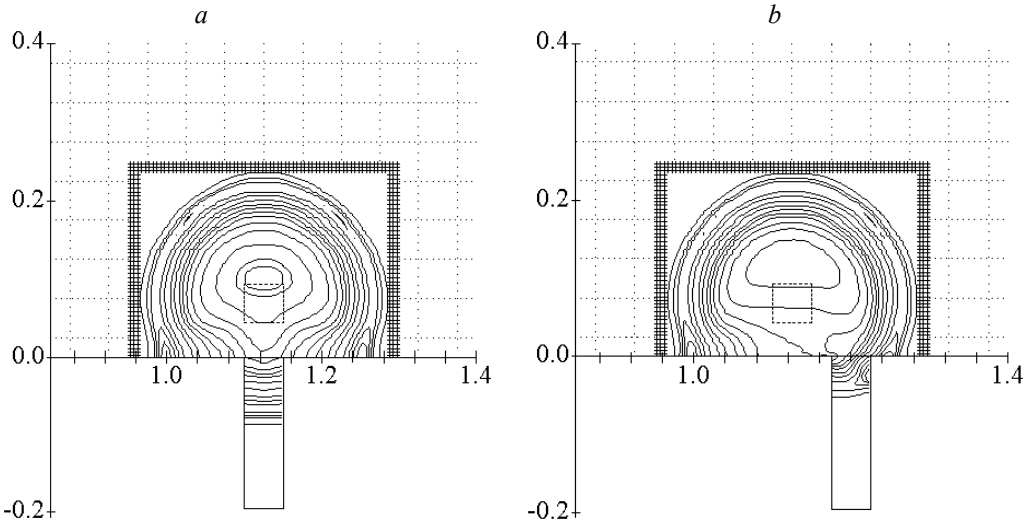

Fig. 2.

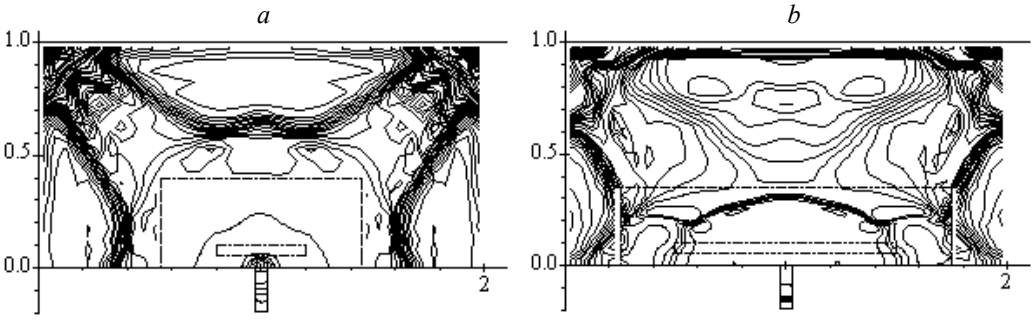

Fig. 3.

time practically monotonously. However, if the pneumatic route is not long, the pressure oscillations were observed.

Some auto-oscillating regime was state in the duct. In the considered case, one wave length is nearly equal to the narrow duct length $d_k = 0.2$. The gas movement is two-dimensional. Firstly, the shock wave entered into the duct and propagating along it is straight (for the conditions of the main variant, see Fig. 1, *a* and 2, *a*). But, in time, even in this case two-dimensional effects are developed. It may be seen from Fig. 5, where the pressure distribution for the main variant at the moment of time $t = 1$ is drawn. In the duct the pressure distribution is almost symmetrical relative to a vertical line passing along the channel centerline. Near the side walls the pressure is decreased; near the bottom and at the duct entrance it is higher (Fig. 5 shows the duct regions where the isobars are plotted $p = 9.5, 9.6, 9.8, 10, 10.5, 11$ and 11.5). Fig. 5 shows the plotted isobars outside the duct region from $p = 10$ with a step 0.5 up to 12 and further with a step of 1 up to 16. Unsymmetrical character of the pressure distribution in the chamber is connected with unsymmetrical position of the energy release zone.

Figure 4 shows an average in time pressure and its relative fluctuation (upper and low smooth curves) side by side with the momentum bottom pressure. In the considered variant it is stated and kept equal to $\overline{p} = 14.6$ during a long period of time, here the relative fluctuation of pressure is equal to $\delta p = 1$.

Essential difference between the average bottom pressure and the mean pressure in chamber should be taken into consideration. The last is equal to $\langle p \rangle = 13.52$ (upper curve), and the relative fluctuation is $\delta p = 0.13$ (low curve), as it may be seen from Fig. 6. This value $\langle p(t) \rangle$ differs from the initial value $\langle p(0) \rangle$ in 0.7 % ($\langle p(0) \rangle = 13.44$).

In the different parts of the chamber an average pressure $\overline{p}$ is also close to the mean in volume value $\langle p \rangle$. It is seen from Fig. 7, in which the numerals point the curves of dependence of pressure on time: 1 is mean in volume $\langle p \rangle$, 2 ÷ 6 is averaged in time $\overline{p}$ in the points with the coordinates (*x, y*) accordingly: (0.25; 0), (0; 0.5), (0.25; 1), (1; 1), (2; 0.5), 7 is at the narrow duct enter, 8 – at its bottom. Thus, whereas the pressure in the chamber is more or less levels off, the pressure in the narrow duct and adjoined chamber zone is higher in the mean and its dispersion is significant (see Fig. 4).

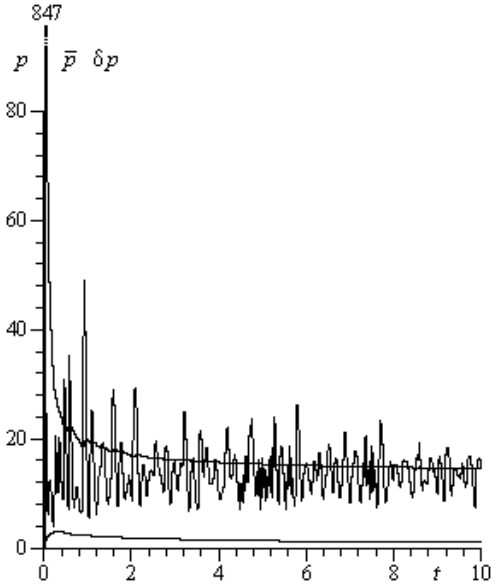

Fig. 4.

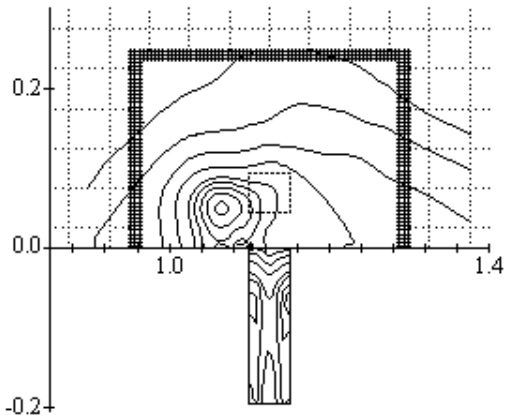

Fig. 5.

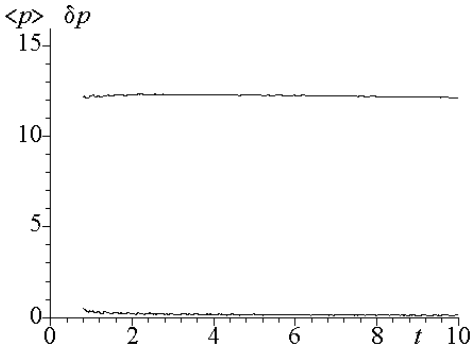

Fig. 6.

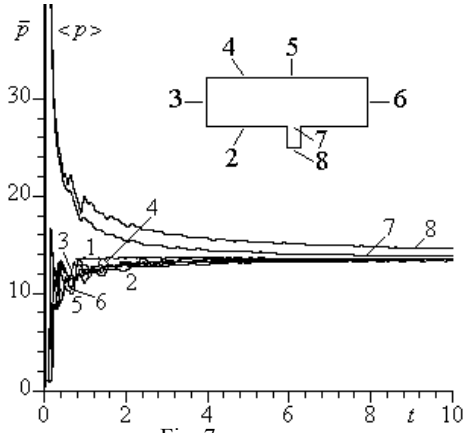

Fig. 7.

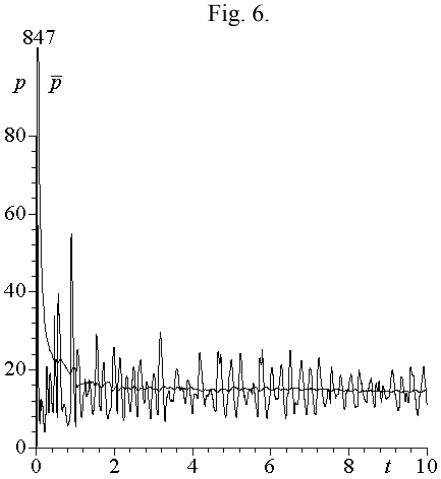

Fig. 8.

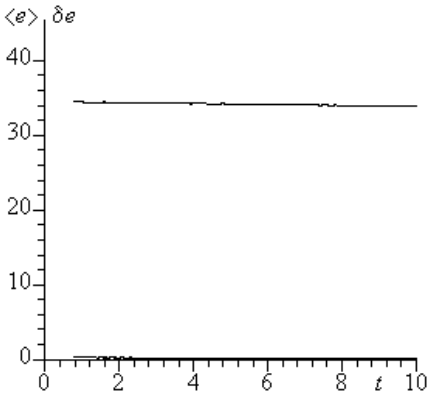

Fig. 9.

At the same time, it should be taken into account that the pressure measured in the experiments is averaged in some period of time which is connected with the measurement equipment. In calculations this period of time must be considered as an additional parameter. Figure 8 presents the results shown in Fig. 4 after recalculation of the mean values using a time period which is equal to $\Delta t = 1$. A significant excess of the bottom pressure averaged by such method over the mean in volume pressure remains: $\bar{p} \sim 14.55$, but the relative fluctuation becomes essentially lower: $\delta p \sim 0.2$.

Figure 9 shows a change in time of the total energy mean value of the gas volume unit $\langle e \rangle$ and its relative fluctuation δe (upper and low curves accordingly). Difference of $\langle e(t) \rangle$ at $t = 10$ on $\langle e(0) \rangle$makes up the value which is not more than 1 %. Comparison of the results presented in Fig. 6 and 9 shows that contribution of kinetic energy into the total energy at large times is slight.

Dispersion of the gas density ρ in a long period of time remains significant. It may be seen in Fig. 10 which shows a change in time of the relative fluctuation of density δρ for different energy release zone lengths by the same quantity of the energy release $\Delta E = 62.5$: curve 1 corresponds to $\Delta x = 0.05$, curve 2 to $\Delta x = 0.2$, 3 to 0.5 and 4 to 1. Dependence of δρ on Δx has non-monotonous character: by increase of the zone length the relative fluctuation δρ is

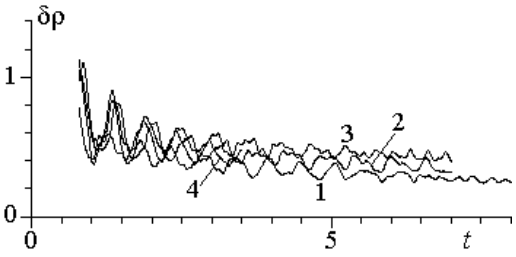

Fig. 10.

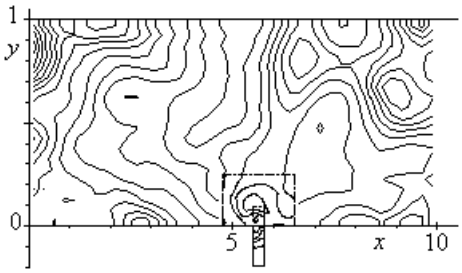

Fig. 11.

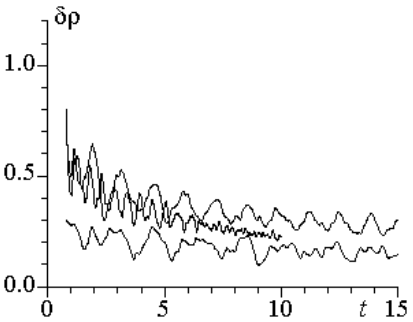

Fig. 12.

increased in the beginning (the supplied energy density decreases; the gas mass which is flying away does not have time to return), then it falls (curve 4 is lower then curve 3). In the moment of time $t = 10$ (the initial pressure in the energy release zone $p = 10000$) the local pressure in the flux region changes approximately by factor of two, and the local density is more then of three. Figure 11 shows for this moment the gas density distribution along the chamber volume. The density levels are presented for the values ρ from 0.6 with a step 0.1 up to ρ = 2 (in the left upper corner of the region). In the narrow duct a minimum value is $\rho \approx 0.6$, in the region extended from the upper wall to the chamber central part a minimum of density is $\rho \approx 0.7$. The density and temperature dispersion should be decreased by increasing of size of the energy release zones keeping the total energy.

The dependence of the relative fluctuation of density on the supplied energy is not monotonous. Figure 12 shows the pattern where the low curve corresponds to the initial pressure in the energy release zone $p = 100$, the upper to $p = 1000$, and the curve within them to $p = 10000$ (the main variant). This is a consequence of the non-linear character of the proceeding processes.

The above mentioned frequency of the bottom pressure oscillations depends on distance of the energy release zone from the low chamber wall (the narrow duct adjoins to this wall), on the depth of the duct, and also on the size of the energy release zone along the axis y (on the value $d_2 - d_1$). Figure 13 shows the dependence of this pressure on time in the main variant (curve (1)), in the variant in which the energy release is posed closer to the low wall ($d_1 = 0.025$) is curve (2), in the variant with less depth narrow duct ($d = 1$) is curve (3) and, at the end, in the variant with $d = 1$, $d_1 = 0.025$, $d_2 = 0.05$ is curve (4). The results in Fig. 13 were obtained for the initial pressure in the energy release zone equal to $p = 10000$. The oscillation frequency of the measured pressure shall decrease by decreasing of the narrow duct depth, of distance from the low wall of the energy release zone and by decreasing of the size $d_2 - d_1$ of this zone.

The above mentioned excess of the averaged bottom pressure over the mean pressure in volume is connected with an effect of anomalous aerodynamic heating. Figure 14 shows a dependence of the averaged in time gas density near the narrow duct bottom (the initial pressure in the energy release zone is $p = 10000$). It is seen that this density is 2.5 times lower than the mean density along the whole volume. This means that the gas temperature near the duct bottom is 2.5 times higher than the mean gas temperature in volume. The effect of anomalous aerodynamic heating essentially depends on thermal conductivity of the gas and the material of the duct walls. This problem should be solved in the context of the Navier – Stocks equations taken into account a wall heat exchange. The results for the case of heat insulation wall will

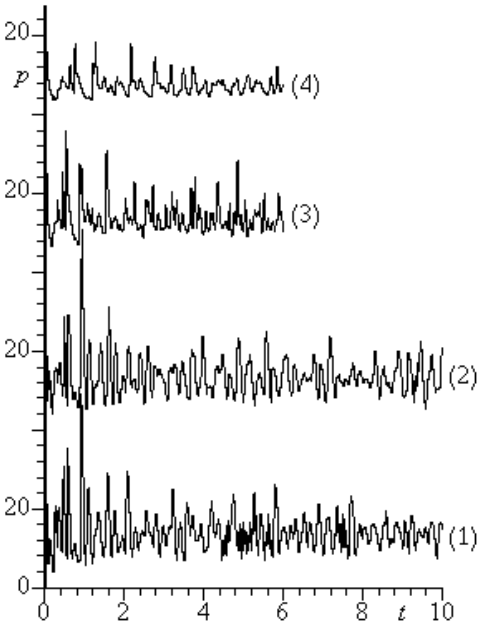

Fig. 13.

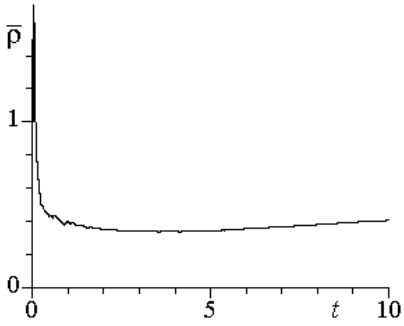

Fig. 14

slightly differ from the results of the given work. Report [5] presented the analogous results where a supersonic gas inleakage on the narrow duct was considered.

It will be possible to restore a true pressure from the results by using the method of paper [6]. For this it is necessary to obtain dynamical characteristics of measurement equipment on a special test bed experimentally.

It seems that account of molecular transfer phenomenon at the flow calculation does not lead to the essential decrease of density and temperature dispersion in the considered interval of time because of relatively low velocities of heat exchange and diffusion.

Results of the given investigation call into question a possibility to use only one measured pressure using probes in the narrow ducts in order to determine the flux parameters in pulse tubes and in the other units with the quickly proceeding processes.

REFERENCES

1. **R.W. Mackormack,** Numerical solution of the interaction of a shock wave with a laminar boundary layer // Lecture Notes in Physics. 1971. Vol. 8. P. 151 – 163.
2. **V.P. Zamuraev,** Numerical modeling of supersonic flow in plane channel with the local source of energy // Intern. Conf. on the Methods of Aerophysical Research: Proc. Pt. 1. Novosibirsk, 1998. P. 239 – 244.
3. **V.P. Zamuraev,** Influence of the local energy release on the supersonic flow in a plane duct // Thermophysics and Aeromechanics. 1999. Vol. 6, No. 3. P. 351 – 360.
4. **V.V. Zatoloka and V.I. Zvegintzev,** Applying of pneumatic routes in drainage experiments of models in impulse regime: Report of ITAM SB RAS, 1975. No. 15313/744. 62 p.
5. **I.E. Ivanov and V.V. Krjukov,** Numerical investigation of non-stationary flows in gas dynamic igniter, The 8th All-Russian Congress on Theoretical and Applied Mechanics: Ann. of Report. Perm', 2001. P. 287.
6. **Gounko Yu.P., Kharitonov A.M., Latypov A.F. and al.** Technique for determination of heat fluxes and force characteristics of ramjet/scramjet models in a hot-shot wind tunnel // Intern. Conf. on the Methods of Aerophysical Research: Proc. Pt. 3. Novosibirsk, 2000. P. 51 – 56.